Journal of Biomolecular NMR, 10 (1997) 389–396
KLUWER/ESCOM

J-Bio NMR 475

Fast-HMQC using Ernst angle pulses: An efficient tool for screening of ligand binding to target proteins

Alfred Ross*, Michael Salzmann and Hans Senn

F. Hoffmann-La Roche AG Pharma Research (PRPI-S), 65/512, CH-4070 Basel, Switzerland

Received 2 June 1997
Accepted 17 July 1997

Keywords: Ernst angle; HMQC; Screening (SAR); Ligand binding; SH3

Summary

The application of Ernst angle pulses in multidimensional NMR spectroscopy is theoretically and experimentally investigated. Theory shows that only for a few pulse sequences employed at high repetition rate, a remarkable gain in sensitivity is possible using Ernst angle pulses. As an example, a new variant of the heteronuclear multiple quantum coherence (HMQC) experiment, the fast-(^{1}H,^{15}N)-HMQC, is described. This sequence allows, with a 1 mM protein sample in H_2O, the acquisition of a highly resolved two-dimensional (^{1}H,^{15}N) correlated spectrum within 37 s. The high efficiency of the fast-HMQC to detect ligand binding to a target protein is demonstrated.

Introduction

The discovery of pharmaceutically active compounds typically starts with the screening for the binding of the molecules in a chemical library or natural products to target molecules. In a second step the properties of the identified compounds are optimized through the synthesis of structurally related analogs. Combinatorial chemical methods using parallel synthesis have considerably increased the number and varieties of compounds to be tested in a screening system (Boutin et al., 1996). In the future, new target proteins are expected to be identified at a rapid pace by the vastly growing genomic information deposited in databases. However, the development of protocols and functional assays to screen the libraries and to identify active compounds is frequently difficult, time-consuming and costly.

NMR spectroscopy is ideally suited to detect weak or strong binding of low-molecular-weight compounds to target proteins. In favorable cases, homonuclear 1D or 2D NMR can be used for the detection of binding sites of proteins (Craik and Higgins, 1989). The use of ^{15}N-labeled protein is particularly advantageous since the observation of ^{15}N- or ^{1}H-amide chemical shift changes in 2D heteronuclear correlation spectra allows an extremely sensitive and efficient determination of ligand binding (Wang et al., 1992; Byeon et al., 1993; Rizo et al., 1994). Because of the ^{15}N spectral editing, no signal from the ligand is observed. Thus, specific but weak binding of low-affinity compounds can be detected in the presence of high ligand concentrations. This is an important advantage over screening assays using fluorimetric or calorimetric detection schemes, where high ligand concentrations can give rise to large background signals. Moreover, the binding location on the protein can be determined once the protein spectrum has been assigned (Wüthrich, 1986). The present molecular size limit of a target protein for NMR detection and structural interpretation of ligand binding is approximately 30 kDa. There are many small target proteins and protein domains which fit this criterion and its number will grow as the size limit is increased by new deuterium-labeling techniques (Venters et al., 1995).

Two conditions must be fulfilled for NMR to be applicable for 'SAR screening' (Shuker et al., 1996): (i) large quantities of ^{15}N-labeled protein must be available for the preparation of NMR samples; and (ii) the measurement time for NMR data acquisition must be short.

In this publication we embark on condition (ii) to improve and develop an NMR experiment for very fast detection and screening of ligand binding to target pro-

*To whom correspondence should be addressed.

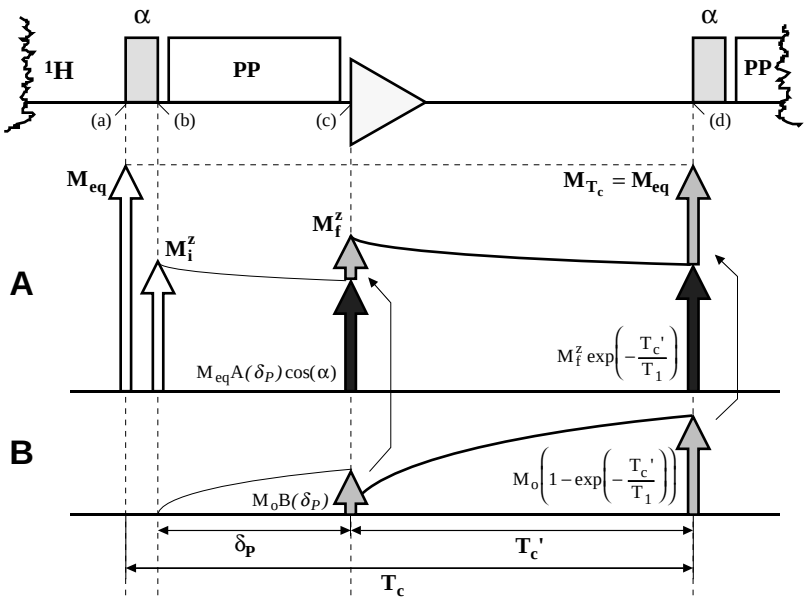

Fig. 1. Relaxation terms during an arbitrary NMR pulse sequence PP using an excitation pulse of flip-angle α. The magnetization M_{eq} present at time point (a) is tilted by the excitation pulse. The z-component of the resulting magnetization is given by M_i^z. During the arbitrary sequence of pulses and delays between time points (b) and (c), M_i^z relaxes according to $M_{eq}A(\delta_P)\cos(\alpha)$ as is indicated in (A). The contribution from the back relaxation to thermal equilibrium is described by $M_0B(\delta_P)$ in (B). Both terms add up to the final z-magnetization M_f^z at time point (c) before acquisition. During the acquisition time and the delay until the first pulse of the next scan, M_f^z relaxes as is indicated in (A). The contribution from back relaxation to thermal equilibrium has to be added, yielding the equilibrium magnetization $M_{T_c} = M_{eq}$ at time point (d).

teins. The recent introduction of pulsed field gradients (PFGs) to high-resolution NMR removed extensive phase cycling and offered the possibility of efficiently recording 2D homo- and heteronuclear correlation spectra (Marion et al., 1989). Here, the application of Ernst angle pulses in multidimensional NMR spectroscopy is investigated (Ernst, 1966). An adapted (^{1}H,^{15}N) correlation experiment (Müller, 1979; Bodenhausen and Ruben, 1980; Bax et al., 1983), the fast-(^{1}H,^{15}N)-HMQC, is described, which allows very high repetition rates with high-quality solvent suppression combined with optimized sensitivity due to excitation pulses under Ernst conditions (Ernst, 1966). The improvement of the solvent suppression proposed for the fast-HMQC still holds true when conventional interscan delays are used. The repetition rate of the fast-(^{1}H, ^{15}N)-HMQC is only limited by the duty cycle of the amplifiers in use, allowing the acquisition of a highly resolved 2D (^{1}H,^{15}N) correlated spectrum within less than 1 min.

In the next section, the theory for Ernst angle pulses when applied to multidimensional pulse sequences is outlined. A criterion for the applicability of Ernst angle excitation to improve sensitivity is evaluated. We show that for the HMQC (Müller, 1979; Bax et al., 1983) and J-spectroscopy (Aue et al., 1976a,b; Macura and Brown, 1985) experiment, the application of a non-90° excitation pulse results in a significant gain in sensitivity if the sequence is applied at very high repetition rate or run on a compound with a long T_1 relaxation time. In the Results section, the application of the fast-HMQC experiment to detect ligand binding to a protein is demonstrated.

Theory

The repetition rate of an NMR pulse sequence depends on the delay T_c between the first pulse of one scan to the first pulse of the next scan. If the spin system is saturated by fast rf pulsing, short interscan delays (T_c) lead to a significant loss in signal intensity. Ernst and co-workers developed an elegant technique to optimize the sensitivity in fast pulsed 1D one-pulse NMR experiments by the application of a non-90° flip-angle (Ernst et al., 1987), known as the Ernst angle (Traficante, 1992; Cavanagh et al., 1996). Optimized sensitivity for an interscan delay T_c, and longitudinal relaxation time T_1, is obtained by the application of an excitation angle α_{ernst} given by

$$\cos(\alpha_{ernst}) = \exp(-T_c/T_1) \quad (1)$$

The longitudinal equilibrium magnetization M_{eq} in dependence of the thermal equilibrium magnetization M_0 is

$$M_{eq} = M_0 \frac{\left(1-\exp\left(-T_c/T_1\right)\right)}{\left(1-\exp\left(-2T_c/T_1\right)\right)} \quad (2)$$

Transfer of transverse magnetization from one scan to the next has been neglected, an assumption justified for macromolecular samples. The signal resulting from a single rf pulse applied to M_{eq} with a flip-angle α_{ernst} is calculated as

$$\text{Signal} = M_{eq}\sin(\alpha_{ernst}) \quad (3)$$

and the signal-to-noise ratio per measurement time, referred to as the sensitivity of the single pulse experiment, is (Ernst et al., 1987)

$$\text{Sensitivity} = \text{Signal}/\sqrt{T_c} \tag{4}$$

In the case of multidimensional or multipulse experiments, the evaluation of optimized conditions proceeds as follows (Fig. 1): assuming that the first pulse of the experiment is performed as a non-90° x-pulse of flip-angle α, the magnetization M_{eq} at time point (a) is transformed to

$$\begin{aligned}\vec{M}_i &= M_{eq}(\sin(\alpha)\vec{e}_y + \cos(\alpha)\vec{e}_z) \\ &= M_i^y\vec{e}_y + M_i^z\vec{e}_z\end{aligned} \tag{5}$$

An arbitrary sequence of pulses and delays of total length δ_P between time points (b) and (c) in Fig. 1 converts the z-component of the initial magnetization (M_i^z) to a final amplitude M_f^z, which can be parametrized as follows:

$$M_f^z = M_{eq}A(\delta_P)\cos(\alpha) + M_0B(\delta_P) \tag{6}$$

The constant $A(\delta_P)$ summarizes the transfer of M_i^z during δ_P due to the applied pulses and delays, whereas the back relaxation to thermal equilibrium during (b) and (c) is combined in $B(\delta_P)$. The relaxation behavior of these two components is schematically drawn below the pulse scheme of Fig. 1. During the acquisition time and the delay until the first pulse of the next scan at time point (d), the deviation from the equilibrium magnetization $\Delta M^z = (M_0 - M_f^z)$ relaxes according to $\exp(-T_c'/T_1)$. Thus, the longitudinal magnetization M_{T_c} at time point (d), which equals the equilibrium magnetization M_{eq}, is

$$M_{T_c} = M_{eq} = M_0 - (M_0 - M_f^z)\exp(-T_c'/T_1) \tag{7}$$

M_{eq} is found by simple mathematics as

$$M_{eq}(\alpha, \delta_P, T_c', T_1) = M_0\frac{\left(1-\exp(-T_c'/T_1)+B(\delta_P)\exp(-T_c'/T_1)\right)}{\left(1-A(\delta_P)\exp(-T_c'/T_1)\cos(\alpha)\right)} \tag{8}$$

Insertion of Eq. 8 into Eq. 3, calculating the derivative with respect to α, and setting the corresponding expression equal to zero results in

$$\cos(\alpha) = A(\delta_P)\exp(-T_c'/T_1) \tag{9}$$

The solution of this equation is thus the Ernst angle α_{ernst} for the given experiment. This angle is only dependent on $A(\delta_P)$, which can be readily explained by the following considerations: if there is only back relaxation to thermal equilibrium, expressed by $B(\delta_P)$, but no transfer of initial z-magnetization to the next scan ($A(\delta_P)=0$), the excitation angle to obtain maximum signal intensity simply is 90° (Eq. 9), and the equilibrium magnetization M_{eq} is only determined by the thermal equilibrium magnetization M_0 (Eq. 7).

The two parameters $A(\delta_P)$ and $B(\delta_P)$ can be calculated in dependence of the architecture of the applied pulse sequence. Note: In non-constant-time experiments both parameters change by incrementing evolution periods within the sequence. In addition, they depend on the phases of the pulses. Thus, the application of quadrature detection based on TPPI (Marion and Wüthrich, 1983) or States (States et al., 1982) might influence both parameters.

In the following, multidimensional NMR experiments will be classified according to their dependence on the parameters $A(\delta_P)$ and $B(\delta_P)$. We will focus on experiments where the excited nucleus is the same as that detected, i.e. any $^1H,^1H$ correlation or any $X,^1H$ correlation using a forth and back magnetization transfer step. Cases where phase cycling changes the parameters $A(\delta_P)$ and $B(\delta_P)$ from scan to scan will be excluded, since in most cases phase cycling can be entirely replaced by gradient-based coherence selection (Barker and Freeman, 1985; Brereton et al., 1991; Ross et al., 1993,1996).

90° Excitation pulse

It is shown by Eq. 9 that the excitation pulse giving highest sensitivity is 90° if $A(\delta_P) = 0$. In the following, we discuss examples of practical interest where this is fulfilled:

(1) In the COSY sequence (Jeener, 1971; Aue et al., 1976a,b), z-magnetization present after the first pulse is flipped to the xy plane by the second 90° detection pulse prior to acquisition. M_f^z and $A(\delta_P)$ become zero.

(2) In pulse sequences using long high-frequency pulsetrains, z-magnetization remaining after the first pulse is strongly reduced by saturation effects and/or dephasing due to B_1 field inhomogeneity. This is the case for any type of TOCSY mixing sequence (Braunschweiler and Ernst, 1983; Bax and Davis, 1985a,b), experiments utilizing composite pulse decoupling (cpd) on the excited and detected spin (Shaka and Keeler, 1987), and ROESY-type experiments (Bothner-By et al., 1984; Bax and Davis, 1985a,b). In these cases no advantage is expected using non-90° excitation pulses.

(3) If M_i^z is flipped transverse during long delays, transverse relaxation serves (if applied on a macromolecular sample) for the fast decay of the contribution proportional to $A(\delta_P)$. Again no notable advantage using non-90° excitation pulses is expected. This is e.g. the case in experiments using a NOESY (Jeener et al., 1979; Bodenhausen et al., 1984) mixing time. The second 90° pulse of the sequence flips M_i^z to the transversal plane. During the mixing time in the 100 ms range, this transverse magnetization relaxes efficiently. The same holds true for hetero-

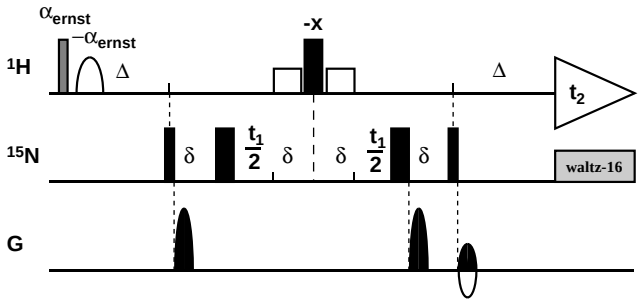

Fig. 2. Pulse sequence for the fast-HMQC. Narrow rectangles denote 90° pulses and broad rectangles denote 180° pulses. The first hard pulse is applied with an Ernst flip-angle α_{ernst}. The following 2 ms sinc-shaped pulse of flip-angle $-\alpha_{ernst}$ flips the water back to the +z-axis (Grzesiek and Bax, 1993). The WATERGATE (Piotto et al., 1992) for solvent suppression is placed in the middle of the evolution period, producing a net 0° rotation for the water magnetization. The soft pulses were rectangular pulses of length 1 ms. All pulses are applied with phase +x except for the 180° pulse in the middle of the evolution period, which is applied with phase −x. The delays were chosen as follows: $\Delta = 5.2$ ms, $\delta = 1.4$ ms. The first two gradients both have a length of 1 ms with a strength of 25 G cm^{-1}, and the third gradient is applied for 1 ms with a strength of 4.87 G cm^{-1}. Phase-sensitive detection in t_1 is achieved using echo–antiecho selection by inverting the sign of the third gradient (Barker and Freeman, 1985; Brereton et al., 1991).

nuclear modifications of the sequence like HSQC-NOESY (Fesik and Zuiderweg, 1988).

For all examples described above, the optimum angle is 90°, and the sensitivity is given using Eq. 8 as

$$\text{Sensitivity} = M_0 \frac{1-\exp(-T_c'/T_1)}{\sqrt{T_c}} \qquad (10)$$

Optimized T_c for this class of experiments is calculated by setting the derivative of Eq. 10 equal to 0. If $\delta_P \ll T_c'$ is assumed, the result is

$$2T_c'/T_1 = \exp(T_c'/T_1) - 1 \qquad (11)$$

The solution of this transcendental function is given by $T_c' \approx 1.25 T_1$.

In another class of experiments, $A(\delta_P)$ strongly depends on the length of an incremented delay of the multidimensional experiment due to chemical shift evolution or relaxation effects. Thus, it is not possible to define a unique Ernst angle optimizing the sensitivity of the experiment for all increments. An example is the HSQC sequence (Morris and Freeman, 1979; Bodenhausen and Ruben, 1980; Burum and Ernst, 1980). Here M_i^z is flipped in the transversal plane during the precession period of the heteronucleus. If applied to a macromolecular sample, fast T_2 relaxation causes the situation described above. In contrast, in the HMQC experiment M_i^z is aligned along the z-axis during the precession of the heteronucleus. Only a small decay due to T_1 relaxation is seen.

Based on the given examples, one has to investigate carefully whether the application of Ernst angle pulses is a promising strategy for a given sequence.

Ernst angle excitation pulse

We want to focus on pulse sequences, where besides the initial Ernst angle pulse only net 0° or 180° pulses are applied on the excited/detected spin. In these sequences, neither $A(\delta_P)$ nor $B(\delta_P)$ are necessarily close to zero. Examples are J-spectroscopy (Aue et al., 1976a,b; Macura and Brown, 1985) and the HMQC sequence (Müller, 1979; Bax et al., 1983) used to achieve heteronuclear shift correlation spectra.

As an application, the parameters $A(\delta_P)$ and $B(\delta_P)$ will be calculated for the HMQC sequence shown in Fig. 2. The summation of all delays (legend to Fig. 2) results in an effective duration $\delta_P = t_1 + 2\Delta + 4\delta$ (see the Appendix):

$$A(\delta_P) = \cos(\beta)\exp(-\delta_P/T_1) \qquad (12)$$

$$B(\delta_P) = (1-\exp(-\delta_P/2T_1))(1+\cos(\beta)\exp(-\delta_P/2T_1)) \qquad (13)$$

The offset dependence of the selective pulses used is accounted for by the effective flip-angle β.

Results

To demonstrate the effect of non-90° excitation pulses on the sensitivity of multidimensional NMR experiments run with high repetition rates, we designed the fast-HMQC experiment shown in Fig. 2. The first proton pulse is applied under Ernst conditions using the flip-angle α_{ernst} determined by the desired repetition rate of the experiment and the spin-lattice (T_1) relaxation time of the molecule, according to Eqs. 9 and 12. After the initial pulse,

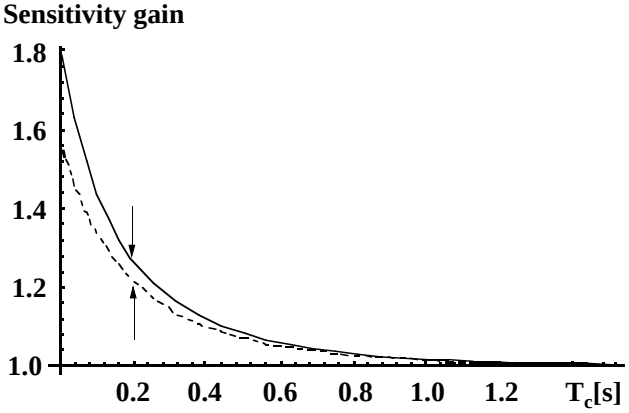

Fig. 3. Sensitivity gain as a function of the repetition time of the fast-HMQC experiment (Fig. 2) by using an excitation pulse under Ernst angle instead of a 90° pulse. The solid line shows the sensitivity gain for the first time increment ($t_1 = 2$ μs) and the dotted line for the last time increment ($t_1 = 24$ ms). The figure was calculated by the use of Eq. 4 in concatenation with Eqs. 3, 8, 9, 12 and 13. As is indicated by the arrows, a gain in sensitivity of 25% is expected for the fast-HMQC setup.

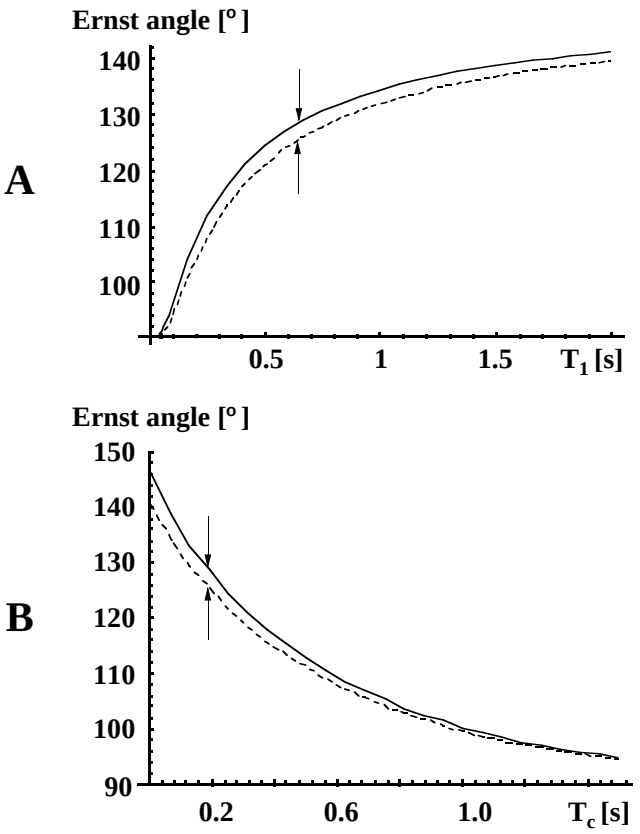

Fig. 4. (A) Dependence of the Ernst angle on the longitudinal relaxation (T_1) is shown for the first ($t_1 = 2$ µs, solid line) and the last time increment ($t_1 = 24$ ms, dotted line) of the fast-HMQC experiment (Fig. 2) using a repetition time of 200 ms. At a T_1 value of 640 ms, found experimentally for the amide protons of SH3 p56^{lck}, the arrows indicate an Ernst angle of 128° for the excitation pulse. (B) Dependence of the Ernst angle on the repetition time is shown at a T_1 of 640 ms. At a repetition time of 200 ms, the expected Ernst angle for the fast-HMQC is 128° as is indicated by the arrows.

the transverse proton magnetization evolves during $\Delta = (2\ ^1J(^1H,^{15}N))^{-1}$ to antiphase coherence with respect to ^{15}N. In order to prevent the saturation of water magnetization in the course of the experiment and, thus, to minimize saturation transfer to the amide protons (Grzesiek and Bax, 1993), the water magnetization is immediately flipped back to the +z-axis by the selective soft pulse following the ^1H excitation pulse. Successively, antiphase protein magnetization is transformed to multiple quantum coherence by the first ^{15}N 90° pulse. The two PFGs, placed in the δ-180°(^{15}N)-δ intervals, offer a twofold advantage: (i) phase-sensitive detection in the F1 dimension is achieved by coherence selection via gradients (Barker and Freeman, 1985; Brereton et al., 1991); and (ii) the WATERGATE (Piotto et al., 1992) for solvent suppression is placed in the middle of the evolution period. Protein magnetization is rephased during the back-transfer to in-phase ^1H magnetization by the third PFG, applied at strength γ_H/γ_N times the sum of the first two gradients. The duty cycle of the amplifiers limits the repetition rate of this experiment to 200 ms, of which 79 ms is required by the t_2 acquisition time and 16.8 ms by the pulse sequence.

The calculated sensitivity of the HMQC experiment (Fig. 2) using an Ernst angle compared to that using a 90° excitation pulse as a function of T_c is shown in Fig. 3. The solid line indicates the first time increment and the dotted line represents the last time increment of the experiment. If the excitation angle of the first pulse is adjusted to the Ernst condition, the sensitivity gain of the experiment utilizing a repetition delay in the 200 ms range is approximately 25% compared to that achieved using a 90° excitation pulse. Comparison of the sensitivity at 200 ms repetition time with Ernst angle pulse to the usual 1 s interscan delay and 90° excitation pulse shows that no sensitivity is lost by running the HMQC in the fast mode (data not shown). Figure 4 shows the Ernst angle of the HMQC experiment (Fig. 2) as a function of T_1 at a repetition time of 200 ms (A). The dependence on the repetition time T_c for a longitudinal relaxation time of 640 ms

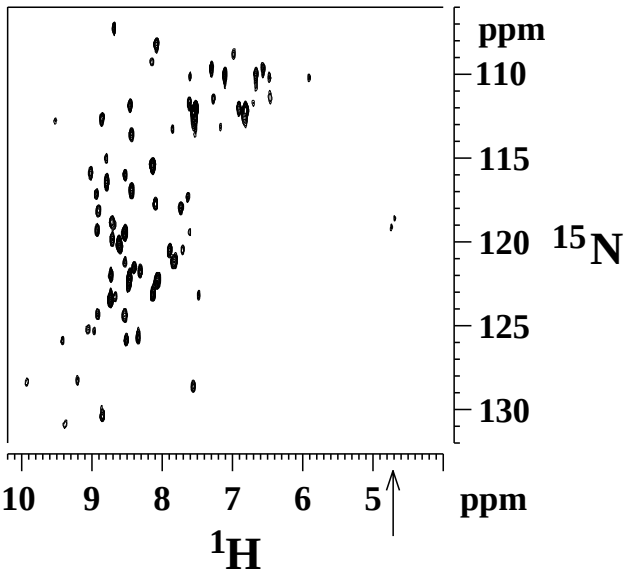

Fig. 5. ($^1H,^{15}N$)-HMQC spectrum recorded with the pulse sequence of Fig. 2 using an Ernst angle for the initial proton pulse of 14.1 µs duration. The total recording time was 37 s using a 1 mM uniformly ^{15}N-labeled sample of the SH3 domain of human p56^{lck} at 298 K. The repetition time of the experiment was 200 ms, given by an acquisition time of 79 ms in t_2, an interscan delay of 104.2 ms, and a duration of the pulse sequence of 16.8 ms. The spectrum was recorded with the following settings: spectral widths of 6024 Hz in the proton dimension and 1320 Hz in the ^{15}N dimension, 512 complex points in the ^1H acquisition and 64 complex points in the indirect dimension. The ^1H transmitter was positioned at 4.7 ppm and the ^{15}N transmitter frequency at 119 ppm. The WALTZ decoupling was employed with a field strength of 2 kHz. Prior to Fourier transformation, the acquired data were multiplied by a quadratic 30° phase-shifted cosine filter in both dimensions and zero-filled. No filter was applied for the suppression of the water resonance, indicated by the arrow at 4.7 ppm. The spectrum was acquired on a Bruker AMX-2 500 spectrometer equipped with a triple-resonance probehead and a self-shielded z-gradient coil.

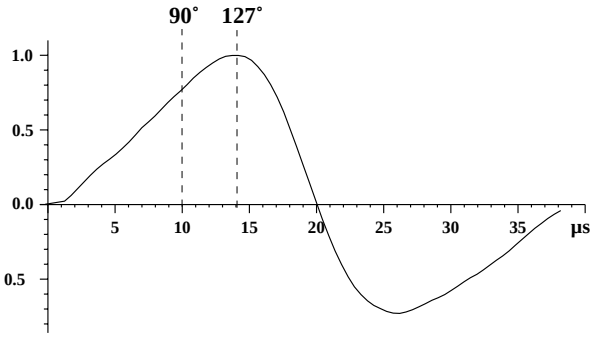

Fig. 6. The Ernst angle is determined with the pulse sequence of Fig. 2 for a repetition time $T_c = 200$ ms by incrementing the duration of the first hard pulse from zero to 40 µs in 0.5 µs steps. The plot shows the behavior of a single NH proton signal of the SH3 domain of human p56^{lck} with increasing flip-angle of the initial hard pulse. The maximum signal amplitude is attained for an Ernst angle of 128° corresponding to a pulse length of 14.1 µs. The 180° pulse has a length of 20 µs, which yields a nominal 90° pulse of 10 µs duration.

is shown in (B). The minor influence of t_1 incrementation on the sensitivity is clearly seen by the small difference between the curve for the first (solid line) and the last time increment (dotted line). The expected Ernst angle for the experimental setup is 128° in both (A) and (B) as is indicated by the arrows.

As an application, the (^{1}H,^{15}N) correlation spectrum of the SH3 domain of human p56^{lck} (Fig. 5) was recorded with the fast-HMQC experiment of Fig. 2 within 37 s. The protein was uniformly ^{15}N-labeled, dissolved in 95% H_2O / 5% D_2O at a concentration of 1 mM. No filter was applied to suppress the water resonance at 4.7 ppm during data processing. Thus, the water suppression achievable for this experiment is state of the art, allowing the most sensitive receiver gain setting available at our spectrometer. All expected cross signals are visible in the spectrum.

The Ernst angle α_{ernst} of the initial proton pulse was determined experimentally by incrementing the initial proton pulse from zero to 40 µs and keeping the ^{15}N t_1 evolution period at a fixed value of 10 µs. Figure 6 shows the time course for the intensity of a resolved NH resonance. The nominal 180° pulse is located at the zero-crossing at 20 µs, whereas the Ernst angle is determined by the maximum intensity at 14.1 µs. This compares to a flip-angle of 128°, nicely demonstrating that the Ernst conditions also apply for macromolecules with relatively short spin-lattice relaxation times. The theoretical value was calculated from the experimentally determined T_1 relaxation time of the amide protons of SH3 p56^{lck} of 640 ms (Markley et al., 1971). Using Eqs. 9 and 12, the Ernst angle is calculated to 128° (Fig. 4A). There is a strong agreement between theory and experiment. A discrepancy of 6° between the theoretical and the experimentally determined Ernst angle is obtained if the off-resonance effect of the water flip-back WATERGATE sequence is neglected. A 150° rather than the exact 180° inversion for the amide region of the spectrum is observed (data not shown). This shows the significant off-resonance effect of the fast-HMQC sequence.

Figure 7 compares the F2 projection of the spectrum shown in Fig. 5 (solid line) to that of a (^{1}H,^{15}N)-HMQC recorded under exactly the same conditions but using a nominal 90° pulse instead of the Ernst angle pulse (dotted line). The tilt-angle for the water flip-back pulse has been adjusted individually for both experiments in order to avoid the saturation of the water magnetization (Grzesiek and Bax, 1993), which would produce a reduction in signal for exchangeable amide protons. As is expected by inspecting Fig. 3, the gain in the signal-to-noise ratio is around 25% on average for the spectrum collected using Ernst angle excitation.

A demonstration for the use of the fast-HMQC experiment for detecting ligand binding to a target protein is shown in Fig. 8. Selected regions from (^{1}H,^{15}N)-HMQC spectra are shown which were acquired before (A) and after (B) adding a peptide ligand to the protein solution of SH3 p56^{lck}. Resonances with distinct chemical shift differences upon binding to the peptide are indicated by the one-letter amino acid symbol and the sequence number. Each spectrum was recorded within 37 s. No readjustment of experimental parameters has been performed after adding the ligand.

We want to emphasize the difference of the achievable sensitivity at a given repetition time compared to the sensitivity possible at an optimized repetition time. For the latter, a significant improvement by optimizing the interscan delay together with the excitation angle of the first pulse is not possible. Based on Eqs. 3, 4, 8, 9, 12 and 13, the optimized repetition time T_c for the longitudinal

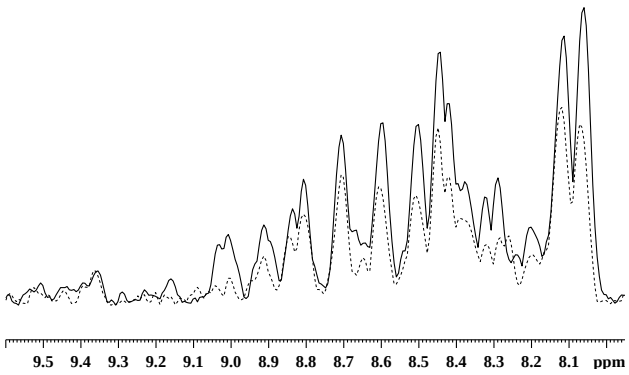

Fig. 7. The F2 projection of 2D (^{1}H,^{15}N)-HMQC spectra of the SH3 domain of human p56^{lck} recorded with the pulse sequence of Fig. 2. The flip-angle of the initial hard pulse was applied at the Ernst angle of 128° (14.1 µs duration) for the spectrum plotted by a solid line, and at the nominal 90° pulse (10 µs) for the spectrum plotted by a dotted line. Both 2D spectra were acquired within 37 s, using the same conditions as for the spectrum of Fig. 2. Prior to Fourier transformation, the acquired data were multiplied by a quadratic cosine filter in both dimensions and zero-filled to 2048 complex points in the proton dimension and to 128 complex points in the indirect dimension.

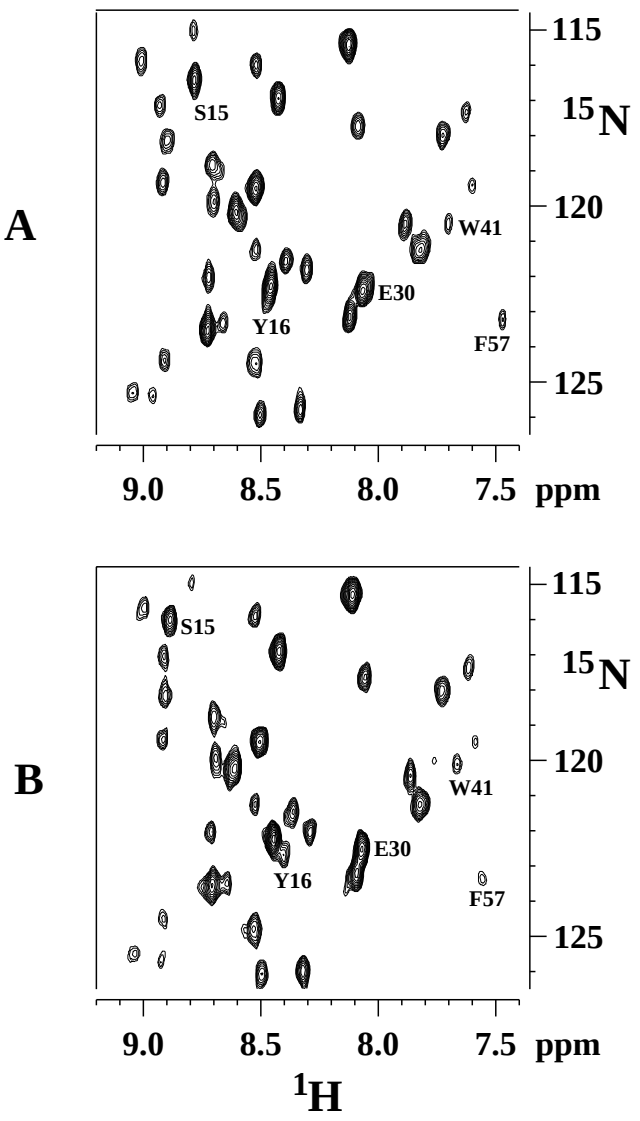

Fig. 8. Regions from the (^{1}H,^{15}N)-HMQC spectra of (A) free SH3 and (B) SH3 complexed to a proline-rich ligand. Both spectra were recorded with the fast-HMQC under the same conditions as the spectrum of Fig. 5 within 37 s. Resonances showing distinct shift deviations upon binding are indicated by the one-letter amino acid symbol and the sequence number.

relaxation rate of SH3 p56^{lck} protein was calculated as 465 ms. The respective Ernst angle is 118°. Using these parameters, an improvement of the 'highest' sensitivity possible of 7% compared to a usual interscan delay of 1 s together with a 90° excitation pulse was calculated.

Conclusions

In this paper, a theoretical analysis of non-90° excitation pulses (Ernst angle pulses) in multidimensional NMR spectroscopy is presented. We describe criteria for the applicability of Ernst pulses to gain sensitivity in dependence of the architecture and repetition rate of the pulse sequence, and the longitudinal T_1 spin relaxation of the molecule.

As an example of a pulse sequence where the application of Ernst angle pulses in a 2D experiment increases the sensitivity, the (^{1}H,^{15}N)-HMQC experiment is analyzed. We show that for molecules having long T_1 (>3 s) a significant gain in sensitivity (approximately 20% compared to the standard setup using 1 s repetition and 90° excitation) can be obtained by optimizing both the Ernst angle and the repetition rate. If the interscan delay has to be kept short (<1 s), e.g. in fast pulsing experiments with very high repetition rates, a much higher gain in the relative sensitivity is achieved in an experiment using optimized Ernst angle excitation versus 90° pulsing. Theoretically, if no interscan delay were employed, a gain of approximately 70% could be realized even for samples having $T_1 < 1$ s. Experimentally, an increase in the relative sensitivity of approximately 25% was obtained due to hardware limitations (duty cycle of the heteronuclear decoupler) which limit the repetition time of the experiment to 200 ms. A 2D (^{1}H,^{15}N) correlation spectrum of a uniformly ^{15}N-labeled 1 mM protein solution can thus be recorded in only 37 s. To circumvent water and amide saturation caused by the fast pulsing, an optimized pulse sequence with state-of-the-art water suppression (fast-HMQC) was developed.

With this experiment the efficient analysis of a large number of samples (e.g. in a binding assay) is feasible. The technique would also be useful for studying protein folding kinetics and chemical exchange processes on the minute time-scale, a time regime which so far has not been accessible by other multidimensional NMR techniques.

It has to be mentioned that the P/N-type selected HMQC approach used here has theoretically an intrinsic loss of sensitivity by a factor of 2 when compared to the gradient-based sensitivity-enhanced HSQC method described in the literature (Kay et al., 1992; Kontaxis et al., 1994). The simplicity of experimental setup and data processing together with insensitivity against short transverse relaxation and B_1 field inhomogeneity make our method an alternative tool, especially when applied to molecules of high molecular weight.

The use of homonuclear multidimensional NMR experiments employed at very high repetition rates for routinely performed NMR analysis of small organic compounds is currently under investigation in our laboratory. In these applications the gain in sensitivity (and experimental time) is expected to be more significant as these experiments are not complicated by short T_1 relaxation or hardware limitations.

Acknowledgements

We would like to thank Roland Hany and Glen Dale for carefully reading the manuscript.

References

Aue, W.P., Bartholdi, E. and Ernst, R.R. (1976a) *J. Chem. Phys.*, **64**, 2229–2246.

Aue, W.P., Karhan, J. and Ernst, R.R. (1976b) *J. Chem. Phys.*, **64**, 4226.

Barker, P. and Freeman, R. (1985) *J. Magn. Reson.*, **64**, 334–338.

Bax, A., Griffey, R.H. and Hawkins, B.L. (1983) *J. Magn. Reson.*, **55**, 301–315.

Bax, A. and Davis, D.G. (1985a) *J. Magn. Reson.*, **63**, 207–213.

Bax, A. and Davis, D.G. (1985b) *J. Magn. Reson.*, **65**, 355–360.

Bodenhausen, G. and Ruben, D.J. (1980) *Chem. Phys. Lett.*, **69**, 185–188.

Bodenhausen, G., Kogler, H. and Ernst, R.R. (1984) *J. Magn. Reson.*, **58**, 370–388.

Bothner-By, A.A., Stephens, R.L., Lee, J.-M., Warren, C.D. and Jeanloz, R.W. (1984) *J. Am. Chem. Soc.*, **106**, 811–813.

Boutin, J.A., Hennig, P., Lambert, P.-H., Bertin, S., Petit, L., Mahieu, J.-P., Serkiz, B., Volland, J.-P. et al. (1996) *Anal. Biochem.*, **234**, 126–141.

Braunschweiler, L. and Ernst, R.R. (1983) *J. Magn. Reson.*, **53**, 521–528.

Brereton, I.M., Crozier, S., Field, J. and Doddrell, D.M. (1991) *J. Magn. Reson.*, **93**, 54–62.

Burum, D.P. and Ernst, R.R. (1980) *J. Magn. Reson.*, **39**, 163–168.

Byeon, I.J., Yan, H., Edison, A.S., Booberry, E.S., Abildgaard, F. and Markley, J.L. (1993) *Biochemistry*, **32**, 2508–2521.

Cavanagh, J., Fairbrother, W.J., Palmer III, A.G. and Skelton, N.J. (1996) *Protein NMR Spectroscopy. Principles and Practice*, Academic Press, San Diego, CA, U.S.A.

Craik, D.J. and Higgins, K.A. (1989) *Annu. Rep. NMR Spectrosc.*, **22**, 61–138.

Ernst, R.R. (1966) *Adv. Magn. Reson.*, **2**, 1–135.

Ernst, R.R., Bodenhausen, G. and Wokaun, A. (1987) *Principles of Nuclear Magnetic Resonances in One and Two Dimensions*, Oxford Science Publications, Oxford.

Fesik, S.W. and Zuiderweg, E.R.P. (1988) *J. Magn. Reson.*, **78**, 588–593.

Grzesiek, S. and Bax, A. (1993) *J. Am. Chem. Soc.*, **115**, 12593–12594.

Jeener, J. (1971) *Ampère International Summer School*, Basko Polje, proposal.

Jeener, J., Meier, B.H., Bachmann, P. and Ernst, R.R. (1979) *J. Chem. Phys.*, **71**, 4546–4563.

Kay, L.E., Keifer, P. and Saarinen, T. (1992) *J. Am. Chem. Soc.*, **114**, 10663–10665.

Kontaxis, G., Stonehouse, J., Laue, E.D. and Keeler, J. (1994) *J. Magn. Reson.*, **A111**, 70–76.

Macura, S. and Brown, L.R. (1985) *J. Magn. Reson.*, **62**, 328–335.

Marion, D. and Wüthrich, K. (1983) *Biochem. Biophys. Res. Commun.*, **113**, 967–974.

Marion, D., Ikura, M., Tschudin, R. and Bax, A. (1989) *J. Magn. Reson.*, **85**, 393–399.

Markley, J.L., Horsley, W.J. and Klein, M.P. (1971) *J. Chem. Phys.*, **55**, 3604–3605.

Morris, G.A. and Freeman, R. (1979) *J. Am. Chem. Soc.*, **101**, 760–762.

Müller, L. (1979) *J. Am. Chem. Soc.*, **101**, 4481–4484.

Piotto, M., Saudek, V. and Sklenář, V. (1992) *J. Biomol. NMR*, **2**, 661–665.

Rizo, J., Liu, Z.P. and Gierasch, L.M. (1994) *J. Biomol. NMR*, **4**, 741–760.

Ross, A., Czisch, M., Cieslar, C. and Holak, T.A. (1993) *J. Biomol. NMR*, **3**, 215–224.

Ross, A., Czisch, M. and Holak, T.A. (1996) *J. Magn. Reson.*, **A118**, 221–226.

Shaka, A.J. and Keeler, J. (1987) *Prog. Magn. Reson. Spectrosc.*, **19**, 47–129.

Shuker, S.B., Hajduk, P.J., Meadows, R.P. and Fesik, S.W. (1996) *Science*, **274**, 1531–1534.

States, D.J., Haberkorn, R.A. and Ruben, D.J. (1982) *J. Magn. Reson.*, **48**, 286–292.

Traficante, D.D. (1992) *Conc. Magn. Reson.*, **4**, 153–160.

Venters, R.A., Huang, C.C., Farmer II, B.T., Trolard, R., Spicer, L.D. and Fierke, C.A. (1995) *J. Biomol. NMR*, **5**, 339–344.

Wang, J.F., Hinkc, A.P., Loh, S.N., LeMaster, D.M. and Markley, J.L. (1992) *Biochemistry*, **31**, 921–936.

Wüthrich, K. (1986) *NMR of Proteins and Nucleic Acids*, Wiley, New York, NY, U.S.A.

Appendix

In the following, we want to calculate the parameters $A(\delta_P)$ and $B(\delta_P)$ given in Eqs. 12 and 13 for the HMQC sequence.

At the end of an initial pulse of flip-angle α remains magnetization $M_{eq}\cos(\alpha)$ aligned along the z-axis. During the following delay of duration $\delta_p/2 = t_1/2 + \Delta + 2\delta$, this magnetization relaxes back to equilibrium according to

$$M_{eq}\cos(\alpha) \rightarrow M_1 = M_{eq}\cos(\alpha)(\exp(-\delta_P/2T_1)) + M_0(1-\exp(-\delta_P/2T_1)) \quad \text{(A1)}$$

M_1 is flipped by an offset-dependent angle β due to the following WATERGATE (Piotto et al., 1992) sequence resulting in magnetization aligned along the z-axis of an amplitude given by $M_1\cos(\beta)$. Residual transverse magnetization is dephased by the following PFGs. The longitudinal part relaxes during the second half of the sequence of length $\delta_p/2$ back to equilibrium as follows:

$$M_1\cos(\beta) \rightarrow M_2 = M_1\cos(\beta)(\exp(-\delta_P/2T_1)) + M_0(1-\exp(-\delta_P/2T_1)) \quad \text{(A2)}$$

Using Eq. A1 together with Eq. A2 results, after resorting according to Eq. 6, in

$$M_2 = M_{eq}\cos(\alpha)\cos(\beta)(\exp(-\delta_P/T_1)) + M_0(1-\exp(-\delta_P/2T_1)) \times (1+\cos(\beta)\exp(-\delta_P/2T_1)) \quad \text{(A3)}$$

This is identical to the result given in Eqs. 12 and 13.